

differences. From the perspective of thermodynamics, we argue that these two systems belong to the same thermodynamic class in that the dynamics of both systems are affected by the supply of chemical energy input from substrates. Our study also clarifies the relationship between the heat dissipation (\dot{Q}) and enhanced diffusivity of the motor using the theoretical framework of nonequilibrium steady state (NESS) thermodynamics^{22–30} and confers thermodynamic insight into how chemical free energy deposited into a molecular system determines its transport properties.

Dependence of Diffusivity on Motor Velocity. Kinesin-1 walks along microtubules, hydrolyzing one ATP per step.^{12,18,31} To model the kinesin's stochastic movement, one can consider a kinetic cycle consisting of N chemically distinct states, where the probability of being in the n th chemical state, $p_n(t)$ ($n = 1, 2, \dots, N$), obeys a master equation (see Figure 1)^{19–21}

$$\frac{dp_n(t)}{dt} = u_{n-1}p_{n-1}(t) + w_n p_{n+1}(t) - (u_n + w_{n-1})p_n(t) \quad (1)$$

with $u_{N+1} = u_n$, $u_N = u_0$, $w_{N+1} = w_n$, $w_N = w_0$, $p_{N+1}(t) = p_n(t)$, and $\sum_{n=1}^N p_n(t) = 1$. Here, $p_n(t) = \sum_{\mu=-\infty}^{\infty} P_{\mu,n}(t)$ where $P_{\mu,n}(t)$ is the probability of being in the n th chemical state at the μ th reaction cycle. The forward and backward hopping rates between the n th and $(n+1)$ th state are denoted as u_n and w_n , respectively. With $p_n(\infty) = p_n^{ss}$, the steady-state flux j along the cycle is expressed as follows:

$$j = u_n p_n^{ss} - w_n p_{n+1}^{ss} = \frac{\prod_{n=1}^N u_n - \prod_{n=1}^N w_n}{\Sigma(\{u_n\}, \{w_n\})} \quad (2)$$

where $\Sigma(\{u_n\}, \{w_n\}) \equiv \prod_{n=1}^N u_n \sum_{n=1}^N r_n$ with $r_n = u_n^{-1} [1 + \sum_{i=1}^{N-1} \prod_{j=1}^i (w_{n+j-1}/u_{n+j})]$.¹⁹ The net flux, j , is decomposed into the forward and backward fluxes as, $j = j_+ - j_-$ where $j_+ = \prod_{n=1}^N u_n / \Sigma(\{u_n\}, \{w_n\})$ and $j_- = \prod_{n=1}^N w_n / \Sigma(\{u_n\}, \{w_n\})$. Both the mean velocity (V) and effective diffusion constant (D) are defined from the trajectories, $x(t)$, that record the position of individual kinesin motors:

$$V = \lim_{t \rightarrow \infty} \frac{d}{dt} \langle x(t) \rangle = d_0 \lim_{t \rightarrow \infty} \frac{d}{dt} \left[\sum_{\mu=-\infty}^{\infty} \mu \pi_{\mu}(t) \right] \quad (3)$$

and

$$D = \frac{1}{2} \lim_{t \rightarrow \infty} \frac{d}{dt} (\langle (x(t))^2 \rangle - \langle x(t) \rangle^2) \\ = \frac{d_0^2}{2} \lim_{t \rightarrow \infty} \frac{d}{dt} \left[\sum_{\mu=-\infty}^{\infty} \mu^2 \pi_{\mu}(t) - \left(\sum_{\mu=-\infty}^{\infty} \mu \pi_{\mu}(t) \right)^2 \right] \quad (4)$$

where $\pi_{\mu}(t) = \sum_{n=1}^N P_{\mu,n}(t)$ and d_0 is the step size. Both V and D are fully determined in terms of a set of rate constants, $\{u_n\}_{n=1, \dots, N}$ and $\{w_n\}_{n=1, \dots, N}$ ^{20,21} (see the Supporting Information). Regardless of the nature of dynamical process (equilibrium or nonequilibrium, passive or active, biased or unbiased), the first line of eq 4 is the general definition of diffusion constant. Most experiments directly calculate the value of D from trajectories based on eq 4 or at least extract the value of D from formulas derived based on eq 4 (e.g., autocorrelation function of FCS by assuming the normal diffusion⁵).

When [ATP] is the only control variable, a simple relationship between V and D is derived by assuming that

$u_1 (= u_1^0 [\text{ATP}])$ is the only ATP-dependent step in the reaction scheme (Figure 1). Because V and D are both functions of [ATP],^{20,21} it is possible to eliminate the common variable [ATP] (or more conveniently u_1) from the two quantities. For the general N -state model, one can express D as a third-degree polynomial in V (see the Supporting Information for $N = 1$ and 2 and the details of derivation for the N -state model):

$$D(V) = D_0 + \alpha_1 V - \alpha_2 V^2 + \alpha_3 V^3 \quad (5)$$

where α_i 's are the constants, uniquely defined when all the rate constants $\{u_n\}_{n=2, \dots, N}$ and $\{w_n\}_{n=1, \dots, N}$ are known.

This relationship (eq 5) holds as long as a motor particle retaining N internal chemical states walks along 1D tracks which are made of binding sites with an equal spacing. In fact, the enhancement of diffusion in motor particles has also been noted by Klumpp and Lipowsky³² in the name of active diffusion and a similar form of velocity dependent diffusion constant as eq 5 was obtained. The detail of their expression differs from eq 5, however, because the focus of their study was on the effect of the patterns (or geometry) of the underlying scaffold on the active diffusion constant of the motor.

Equation 5 was used to fit the (V , D) data digitized from Visscher et al.'s single molecule measurement on kinesin-1³³ which had reported V and the randomness parameter $r = 2D/d_0V$ ($d_0 = 8.2$ nm, kinesin's step size) at varying load (f) and [ATP]. The fits (dashed line) using eq 5 allow us to determine the parameters D_0 , α_1 , α_2 , and α_3 [see Figure 2A ($f = 1.05$ pN) and Figure 2B ($f = 3.59$ pN)]. As expected, $D(V = 0) = D_0 \approx 10^{-5}$ $\mu\text{m}^2/\text{sec}$ is vanishingly small for kinesin-1 whose motility

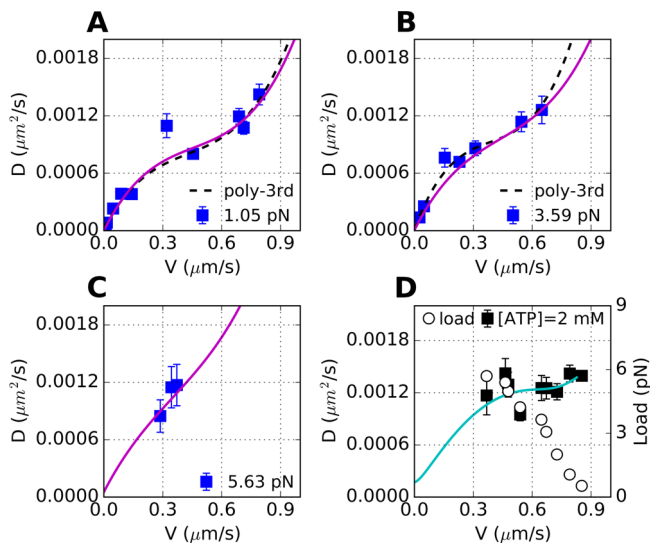


Figure 2. Motor diffusivity (D) as a function of mean velocity (V) of kinesin-1. (V , D) measured at varying [ATP] ($= 0$ – 2 mM) and a fixed (A) $f = 1.05$ pN, (B) 3.59 pN, and (C) 5.63 pN.³³ The standard deviations of D (σ_D) were estimated from $\sigma_D \approx d_0(\sigma_V V + r\sigma_V)$ by using the extracted values of r , V , σ_V , and σ_V . The black dashed lines in panels A and B are the fits using eq 5. For $f = 1.05$ pN and 3.59 pN, (D_0 , α_1 , α_2 , α_3) = (2.2×10^{-5} , 3.8×10^{-3} , 7.1×10^{-3} , 5.5×10^{-3}) and (7.4×10^{-6} , 5.6×10^{-3} , 1.2×10^{-2} , 1.1×10^{-2}), respectively. The solid lines in magenta in panels A–C are plotted using the ($N = 4$)-kinetic model's parameters (Table 2). (D) (V , D) (black filled square) measured at varying f (black empty circle) and [ATP] = 2 mM. The solid line in cyan, plotted by using the parameters in Table 2, is the predicted behavior of $D = D(V)$ when V is varied by f , instead of [ATP].

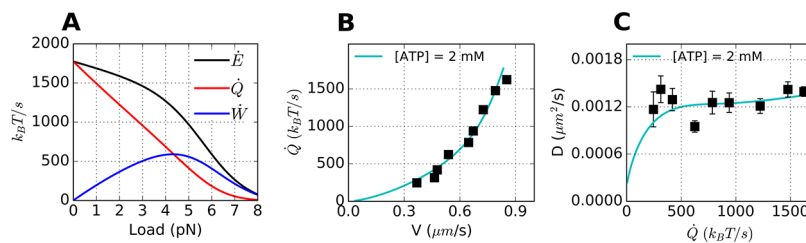


Figure 3. Heat and work production at varying load. (A) Theoretical plot of heat (\dot{Q} , red), work production (\dot{W} , blue), and their sum (\dot{E} , black) as a function of load using ($N = 4$)-state model. (B) Heat production (\dot{Q}) as a function of motor velocity (V), modulated by varying f at $[\text{ATP}] = 2$ mM. (C) D plotted against \dot{Q} when f is varied at $[\text{ATP}] = 2$ mM. The solid lines in cyan are theoretical predictions using the parameters determined in the ($N = 4$)-state model.

is tightly coupled to ATP. At $V = 0$, the flux along the cycle vanishes ($j = 0$), establishing the detailed balance (DB), $u_n p_n^{\text{eq}} = w_n p_{n+1}^{\text{eq}}$ for all n 's with $\sum_{n=1}^N p_n^{\text{eq}} = 1$. In this case, $D_0 = d_0^2 / \sum_{n=1}^N (u_n p_n^{\text{eq}})^{-1} \leq u_{\min} d_0^2 / N$,³⁴ where $u_{\min} = \min\{u_n | n = 1 \dots N\}$. For $[\text{ATP}] \ll 1$, it is expected that $u_{\min} \approx u_1 = u_1^0 [\text{ATP}] \ll 1$.

We also used the ($N = 4$)-state kinetic model by Fisher and Kolomeisky²¹ and determined a set of parameters, $\{u_n\}$, $\{w_n\}$, and $\{\theta_n^{\pm}\}$ (with $n = 1, \dots, 4$), which best describe the kinesin's motility data, by simultaneously fitting all the data points in Figures 2A–C and 5 (see Analysis of Kinesin-1 Data Using ($N = 4$)-State Kinetic Model). For a consistency check, we overlaid a theoretically predicted line (Figure 2D, cyan line) over the data (V, D) obtained at varying f but with fixed $[\text{ATP}] = 2$ mM, which we did not use in determining the parameters. $D(V)$, over the range of $0 < V \lesssim 0.3$ $\mu\text{m}/\text{sec}$ (Figure 2D), predicts the behavior of D at high f regime near a stall force.

Energy and Heat Balance of Molecular Motor. The movement of a molecular motor is driven by a net driving force due to ATP hydrolysis and opposed by the resisting load f . In a NESS, the flux ratio, $K(f) = j_+(f)/j_-(f)$, defined for unicyclic reaction cycle for kinesin, is balanced with the chemical potential difference driving the reaction $\Delta\mu_{\text{eff}}(f)$ (or the affinity $\mathcal{A} = -\Delta\mu_{\text{eff}}$) as

$$K(f) = \frac{\prod_{n=1}^N u_n(f)}{\prod_{n=1}^N w_n(f)} = \exp(-\Delta\mu_{\text{eff}}(f)/k_B T) \quad (6)$$

where $\Delta\mu_{\text{eff}}$ is contributed by chemical potential due to ATP hydrolysis $\Delta\mu_{\text{hyd}}$ and mechanical work (fd_0) against the load f . With $j(f)$ denoting the total flux (i.e., the number of cycles per a given time) at force f , the heat dissipated at a steady state, $\dot{Q} = j(f) \times (-\Delta\mu_{\text{eff}})$, is balanced with the (free) energy consumption $\dot{E} = j(f) \times (-\Delta\mu_{\text{hyd}})$ subtracted by the work against an external load $\dot{W} = j(f) fd_0$; thus

$$\begin{aligned} \dot{Q} &= j(f) \times (-\Delta\mu_{\text{eff}}(f)) = (j_+(f) - j_-(f)) k_B T \log \left(\frac{j_+(f)}{j_-(f)} \right) \\ &= j(f) \times (-\Delta\mu_{\text{hyd}} - fd_0) = \dot{E} - \dot{W} \end{aligned} \quad (7)$$

where \dot{Q} , analogous to the electric power produced by means of current \times voltage, is always positive ($\dot{Q} \geq 0$) regardless of whether $j(f) > 0$ or $j(f) < 0$. Equation 7 is readily obtained by assuming barometric dependence of rates on forces as $u_n = u_n^0 \exp(-f d_0 \theta_n^+ / k_B T)$ and $w_n = w_n^0 \exp(f d_0 \theta_n^- / k_B T)$ with $\sum_{n=1}^N (\theta_n^+ + \theta_n^-) = 1$.^{20,21} When $f = 0$, the motor moves along microtubules unidirectionally but the movement of the motor itself does not perform work to the environment; thus, the entire free energy consumed via ATP hydrolysis ($-\Delta\mu_{\text{hyd}} > 0$)

is dissipated into heat at a rate $j(0) \times (-\Delta\mu_{\text{hyd}})$. When $f \neq 0$, the motor performs work against the load, $W = fd_0$ per cycle. Hence, the total chemical free energy change due to ATP hydrolysis, $-\Delta\mu_{\text{hyd}}$, is dispensed into heat (\dot{Q}) and work (\dot{W}) per cycle, leading to $\dot{E} = \dot{Q} + \dot{W}$.²⁹ Note that $\dot{W} = j(f) fd_0 = 0$ either at $f = 0$ or at the stall condition $f = f_c$, which imposes $j(f_c) = 0$; thus, the work production (\dot{W}) is a nonmonotonic function of f , whereas \dot{E} and \dot{Q} decrease monotonically with f . For concreteness, we plot \dot{E} , \dot{Q} , and \dot{W} as a function of f (Figure 3A). At $[\text{ATP}] = 2$ mM, \dot{W} is maximized at $f \approx 4.5$ pN. The heat production, \dot{Q} , is maximal ≈ 1750 $k_B T/s$ at $f = 0$ and decreases monotonically to zero at stall ($f = f_c$).

The monotonic increase of $\dot{Q}(V)$ (Figure 3B) implies that more heat is generated when the motor moves faster at a smaller f . Higher load (f) that hampers motor movement (smaller V) as in Figure 2D reduces \dot{Q} (Figure 3B). If the dissipated heat does influence the dispersion of the motor, then a positive correlation between \dot{Q} and D should be observed even when both quantities are suppressed at higher force. Indeed, Figure 3C predicts that D increases with \dot{Q} , although the extent of the increase is small over the range where the data are available.

Next, to investigate the effect of varying $[\text{ATP}]$ on V, D , and \dot{Q} , we plotted (V, \dot{Q}) (Figure 4A) and (\dot{Q}, D) (Figure 4B) at

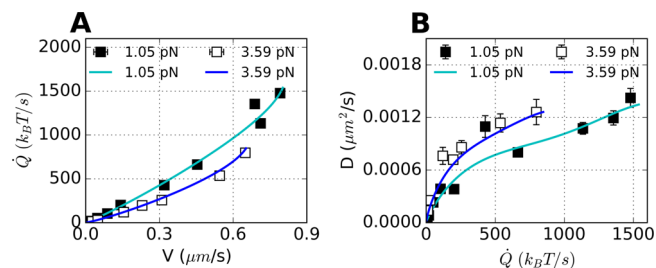


Figure 4. Relationships of \dot{Q} vs V and D vs \dot{Q} modulated under varying $[\text{ATP}]$ but at a constant f . (A) \dot{Q} vs V at $f = 1.05, 3.59$ pN. (B) D vs \dot{Q} at $f = 1.05, 3.59$ pN. Solid lines are the fits using ($N = 4$)-state model with model parameters determined from global fitting of data in Figures 2A–C and 5. The V and D data are digitized from ref 33.

varying $[\text{ATP}]$ with fixed $f = 1.05$ pN or $f = 3.59$ pN. Again, monotonic increase of \dot{Q} with V and the correlation between \dot{Q} and D clearer than that in Figure 3C are observed. Similar to the cubic polynomial dependence of D on V , it is possible to relate V and D with \dot{Q} at constant load. We found that for general N -state model, $\dot{Q} \sim V^2$ and $D \sim \dot{Q}^{1/2}$ at small \dot{Q} (see section 5 of the Supporting Information), which explains the curvatures of the plots at small \dot{Q} regime in Figure 4. From the perspective of NESS thermodynamics,^{22,23} for a motor to

sustain its motility, a free energy cost called *housekeeping heat* should be continuously supplied to the system. For the N -state model, the system relaxes to the NESS from its arbitrary initial nonequilibrium state in a rather short time scale $\tau_{\text{NE}} = 1/\sum_{n=1}^N(u_n + w_n)$ (see section 4 and Figure S2 of the [Supporting Information](#)). In a NESS, the housekeeping heat and the total heat and entropy production discharged to the heat bath are all equal to $\dot{Q} = jk_{\text{B}}T \log(j_+/j_-) \geq 0$ (see section 4 of the [Supporting Information](#)).

Cautionary remarks are in order. Our formalism describing the trajectories of kinesin is based solely on a unicyclic reaction scheme. While straightforward in developing a formalism, the unicyclic reaction scheme leads to a problematic interpretation that the backstep is realized always by a reversal of the forward cycle,²⁴ which means that the backstep near the stall condition is taken with the synthesis of ATP from ADP and P_i . This rather strong assumption could be alleviated by extending the current formalism to the one based on a multicycle model,^{14,24,35,36} so as to accommodate the possibilities of ATP-induced backstep and futile cycle near the stall condition. For the multiple-cycle model, the flux branches into different cycles and the net flux at each kinetic step remains nonvanishing ($j_+ \neq j_-$) even at the stall condition. As a result, it is expected that $\dot{Q} \neq 0$ and $\dot{W} \neq 0$. More explicit calculation of the functional dependence of \dot{Q} or \dot{W} on f , however, requires a detailed model based on a multicycle reaction scheme, which we leave for our future study.

Passive versus Active Particles. Broken DB and violation of the fluctuation dissipation theorem (FDT)^{37,38} differentiate an active system operated under nonconservative forces from a passive system in mechanical equilibrium under conservative forces. For example, the terminal velocity (V) and diffusion constant (D) of a colloidal particle of size R in the gravitational or electric field are mutually independent, so that regardless of V , D is always constant, obeying Stokes–Einstein relation $D \sim D_{\text{SE}} \sim k_{\text{B}}T/\eta R$ where η is the viscosity of media, k_{B} the Boltzmann constant, and T the absolute temperature. A similar argument can be extended to a composite system (e.g., macromolecules in solution) subjected to conservative forces.

In contrast, for a self-propelled active particle, the dependence of diffusivity on its velocity is often noted, and the *effective diffusion constant*, defined as the increment of mean square displacement over time $D_{\text{eff}} = \langle(\delta r)^2\rangle/6t$ at an ambient temperature T , depends on a set of parameters (velocity, density, etc.), violating the FDT.^{39,40} To be specific, let us consider a run-and-tumble motion of a swimming bacterium, which locomotes with a velocity V_b in search of a food. If the mean duration of locomotion is τ_r and the bacterium tumbles occasionally with a rotational diffusion constant D_R for time τ_t , the effective diffusion constant of the bacterium at time t much greater than τ_s and τ_t is estimated to be $D_{\text{eff}} \sim V_b^2\tau_r/6D_R\tau_t$.^{41,42} In this case, V_b or D_{eff} of bacterium is affected not by the ambient temperature but by the amount of food, also violating the conventional FDT (D_{eff} is not $\sim k_{\text{B}}T/\eta R$).^{37,43,44}

Unlike a passive particle in equilibrium, V and D of an active particle are both augmented by the same *nonthermal, nonconservative* force (e.g., ATP hydrolysis). Importantly, regardless of whether a system is in equilibrium or in nonequilibrium, and is passive or active, it is legitimate to *define* the diffusion constant as an increased amount of mean square displacement for time t *without* resorting to the FDT. In ref 5, the signal from FCS measurement was nicely fitted to the

autocorrelation function, $G(\tau)$, which assumed the *normal* diffusive motion of the enzymes.

Comparison of Enhanced Diffusivities between Different Types of Active Particles. While a precise *mechanistic link* between the heat and enhanced diffusion is still elusive in this study as well as in others,^{5–9} our study still offers further insights into the problem of enhanced diffusion of exothermic enzymes.^{1,5} From [Figure 2](#), $(\Delta D/D_0)_{\text{obs}}$ at the maximal velocity of kinesin-1 is as large as $\sim O(10^2)$. For swimming *Escherichia coli*, the enhancement is estimated to be $(\Delta D/D_0)_{\text{obs}} \gtrsim O(10^2)$ (the effective diffusion coefficient of *E. coli* is $D \sim 53 \mu\text{m}^2/\text{s}$ ^{41,45} and $D_0 = D_{\text{SE}} \sim 0.5 \mu\text{m}^2/\text{s}$ by assuming bacterium as a sphere with radius of $0.5 \mu\text{m}$). Considering the extent of enhancement in kinesin-1 and *E. coli*, $(\Delta D/D_0)_{\text{obs}} \sim 0.3–3$ for the substrate fed, exothermic enzymes observed by Riedel et al.⁵ should not be too surprising.

In the framework of unicyclic Markov processes, the diffusion constant (D) in a NESS is defined consistently with [eq 4](#) in terms of forward and backward fluxes (j_+ and j_-). The extent of enhancement in diffusion constant is expressed as (see [eq S41](#))

$$\frac{\Delta D}{D_0} = \frac{j_+ - j_-}{j_0 \log\left(\frac{j_+}{j_-}\right)} - 1 = \left(\frac{j_-}{j_0}\right) \frac{(K-1)}{\log K} - 1 \quad (8)$$

At equilibrium, when the DB is established, $j_+ = j_- = j_0$ (or $K = 1$), which leads [eq 8](#) to $\Delta D/D_0 = 0$. More explicitly, the enhancement of the diffusion constant can be expressed in terms of microscopic rate constants using the ($N = 2$)-state kinetic model (see [eq S9](#) in section 1 of the [Supporting Information](#)), and its theoretical upper bound can be obtained as

$$\frac{\Delta D}{D_0} \leq \left(\frac{\Delta D}{D_0}\right)_{\text{max}} = \frac{u_2^2 + (w_1 + w_2)u_2 - w_1w_2}{2w_1w_2} \quad (9)$$

The inequality in the last line specifies a theoretically achievable upper bound of enhancement $(\Delta D/D_0)_{\text{max}}$, the expression of which remains unchanged even when the passive diffusion component ($D_{\text{SE}} \sim k_{\text{B}}T/\eta R$) is included in D_0 . For a Michaelis–Menten type enzyme reaction, a typical condition, $u_2 \gg w_2$ and $u_2 \simeq w_1$, makes $(\Delta D/D_0)_{\text{max}} \simeq u_2^2/2w_1w_2$ a large number. D (or D_0) itself is a number associated with a squared length scale d_0^2 per unit time. However, the precise meaning of d_0 , a characteristic length, is not clear for the freely diffusing enzymes, while d_0 simply denotes the step size for molecular motors. The dimensionless number, $(\Delta D/D_0)$, eliminates such ambiguity, allowing us to make a direct comparison between 1D transport motors and enzymes.

In the expression $(\Delta D/D_0)_{\text{max}} \simeq u_2^2/2w_1w_2$, u_2 is the key reaction rate that quantifies the catalytic event in the Michaelis–Menten scheme (or “power stroke” in molecular motors). To quantify the enzyme’s efficiency of converting chemical free energy into motion, we define the conversion factor, ψ , as the ratio between the *observed* and *theoretically predicted* enhancement of diffusion constant at the maximal turnover rate ($V = V_{\text{max}}$) as follows:

$$\psi^2 \simeq \frac{\left(\frac{\Delta D}{D_0}\right)_{\text{obs}}}{\left(\frac{\Delta D}{D_0}\right)_{\text{max}}} \quad (10)$$

Table 1. Rate Constants, Enhancement of Diffusion, and Conversion Factor Determined from the ($N = 2$)-State Kinetic Model^a

	Q ($k_B T$)	[S] (mM)	u_1 (s^{-1})	u_2 (s^{-1})	w_1 (s^{-1})	w_2 (s^{-1})	$\left(\frac{\Delta D}{D_0}\right)_{\text{obs}}$	$\left(\frac{\Delta D}{D_0}\right)_{\text{max}}$	ψ
kinesin ($f = 1.05$ pN)	15	2	2200	99	0.55	0.092	6×10^4 (45^{b_c})	9.7×10^4	~ 0.8 (0.02^{b_c})
catalase	40	62	6.2×10^6	5.8×10^4	6.1×10^6	2.2×10^{-13}	~ 1	1.3×10^{17}	$\sim 3 \times 10^{-9}$
urease	24	3	3×10^5	1.7×10^4	2.8×10^5	7.4×10^{-7}	~ 0.3	1.2×10^{10}	$\sim 5 \times 10^{-6}$
AP	17	1.6	1.6×10^5	1.4×10^4	1.5×10^5	4.0×10^{-4}	~ 3	1.9×10^7	$\sim 4 \times 10^{-4}$
TPI	1.2	1.8	1.8×10^5	1.3×10^4	1.7×10^5	4.2×10^3	0.01	1.2	0.09

^aAP, alkaline phosphatase; TPI, triose phosphate isomerase. ^b D_0 determined from the third-degree polynomial fit (eq 5) to the data in Figure 2A was used to estimate $(\Delta D/D_0)_{\text{obs}}$ and ψ .

Mathematically, the factor ψ amounts to the ratio of u_2^{obs}/u_2 , where u_2^{obs} is an actual amount of power stroke; hence, it physically quantifies the extent of chemical energy converted to spatial movement. For kinesin-1 whose ATP-induced conformational dynamics and thermal fluctuations are rectified to a unidirectional movement along a 1D track,¹⁸ a high conversion factor ($\psi \lesssim 1$), i.e., tight coupling between the transitions in chemical state space and motion in real space is expected from the catalytic turnover. In contrast, the lack of scaffold renders the motion of free enzymes in 3D space random and more dissipative; hence, the transitions in chemical state space are weakly coupled to the motion in real space. As a consequence, the extent of conversion from chemical energy to the movement of enzyme is expected to be much lower than that of kinesin-1.

Indeed, we find that $\psi(\text{kinesin}) \gg \psi(\text{freely diffusing enzymes})$. For kinesin-1, $D_{\text{max}} \approx 10^{-3} \mu\text{m}^2/\text{s}$ at $V = V_{\text{max}}$ from Figure 2 and $D_0 = 10^{-8} \mu\text{m}^2/\text{s}$ from the fit to ($N = 2$)-state model (see the Supporting Information) which determines the rate constants u_2 , w_1 , and w_2 lead to $(\Delta D/D_0)_{\text{obs}} \approx 6 \times 10^4$ and $(\Delta D/D_0)_{\text{max}} \approx 7.4 \times 10^5$ from eq 9; therefore, $\psi \approx 0.8$ (or $\psi \approx 0.02$ when $D_0 \approx 2.2 \times 10^{-5} \mu\text{m}^2/\text{s}$ is used from the third-degree polynomial fit: dashed line in Figure 2A). For the cases of Riedel et al.'s exothermic enzymes (catalase, urease, and alkaline phosphatase), whose rate constants are available in Table 1 (or in ref 5), $\psi \sim \mathcal{O}(10^{-4}) - \mathcal{O}(10^{-7})$ is obtained from $(\Delta D/D_0)_{\text{obs}} \sim \mathcal{O}(10^{-1})$ and $(\Delta D/D_0)_{\text{max}} \sim \mathcal{O}(10^7) - \mathcal{O}(10^{17})$.

The net chemical free energy change due to isomerization reaction of substrate (dihydroxyacetone phosphate \rightleftharpoons D-glyceraldehyde 3-phosphate) catalyzed by triose phosphate isomerase would be relatively small ($\Delta\mu_{\text{eff}} \sim 0$ or $K \sim 1$) compared with other highly exothermic enzymes. In this case, it is anticipated from eq 8 that $\Delta D/D_0 \sim 0$. All the values of $(\Delta D/D_0)_{\text{obs}}$, $(\Delta D/D_0)_{\text{max}}$ and ψ discussed here are provided in Table 1.

Direct comparison of the diffusions of kinesin-1 and freely diffusing active enzymes may not appear to be fair. From a perspective of thermodynamics, however, they still belong to the same thermodynamic class in that the motions of both systems require energy input. Furthermore, when mapped on the chemical state space, (enzymatic) activities of both systems are described using Michaelis–Menten relation with ATP concentration. As quantified in the relation of $\psi(\text{kinesin-1}) \gg \psi(\text{freely diffusing enzymes})$, kinesin-1, whose fluctuations are tightly confined on the microtubules, is more efficient in converting thermal/active fluctuations into motion than the freely diffusing enzymes. Thus, our prediction is that confinement of active fluctuations into low dimension leads to a

greater enhancement in diffusivity $(\Delta D/D_0)_{\text{obs}}$, which can be tested for the above-mentioned freely diffusing enzymes by confining them in a narrow nanochannel. Conversely, it is also expected that $(\Delta D/D_0)_{\text{obs}}$ and ψ of free kinesin-1 in solution, i.e., in the absence of microtubules, are reduced greatly to the values less than those for Riedel et al.'s enzymes.

The physical meaning of the term “diffusion constant” used in the literature could be twofold. First, it refers to the response of a system in a solution to thermal fluctuations, which amounts to the diffusion constant defined by the Stokes–Einstein relation, $D_{\text{SE}} = k_B T/\zeta$, where ζ is the friction coefficient. Second, the behavioral random motion of a system being probed is often quantified using the operational definition of diffusion constant, $D_{\text{eff}} = \langle(\delta r)^2\rangle/6t$, at long time limit. In a nondriven thermally equilibrated system, it is expected that $D_{\text{eff}} = D_{\text{SE}}$. However, for a system like swimming bacterium, where unidirectional active motion is randomized with occasional tumblings, there is no reason to expect that the two distinct definitions are inter-related, and $D_{\text{eff}} > D_{\text{SE}}$ should be expected as long as the bacterium is “alive.” It is important to note that in Riedel et al.'s FCS measurement, the behavioral random motion of enzymes was effectively quantified as the diffusivity of the enzymes based on the definition of $D_{\text{eff}} [= \langle(\delta r)^2\rangle/6t]$, and its variation with an increasing turnover rate was extracted from the data fitting to the fluorescence intensity autocorrelation function. Once one accepts that substrate-catalyzing, freely diffusing enzymes are thermodynamically in the same class with molecular motors or swimming bacteria in that all of them are energy-driven (substrate-catalyzing or nutrient-digesting) systems in NESS, the enhancement of enzyme diffusion is no longer enigmatic.

The fundamental difference between passive and active particles is worth highlighting again using Langevin description. In the simplest possible terms, the motion of a passive particle in 1D under an externally controlled field, F_{ext} is described by the Langevin equation $\dot{x}(t) = F_{\text{ext}}/\gamma + \sqrt{2D}\zeta(t)$ where $\zeta(t)$ is the Gaussian noise with $\langle\zeta(t)\zeta(t')\rangle = \delta(t-t')$, which gives rise to the terminal velocity $\langle\dot{x}(t)\rangle = F_{\text{ext}}/\gamma$. In contrast, the corresponding Langevin equation for an active particle is $\dot{x}(t) = V(u, w) + \sqrt{2D(u, w)}\zeta(t)$. In the latter case, both the velocity and diffusion constant at steady state are a function of substrate concentration, $u = u([\text{ATP}])$, the driving force of the particle's motion, which allows us to express D as a function of V such that $D = D(V)$.

To recapitulate, in this study we determined a set of microscopic rate constants, which best describe the “trajectories” of kinesin-1, on a unicyclic kinetic model consisting of N -contiguous chemical states and transition rates between them and evaluated the heat dissipation along the reaction cycle. The

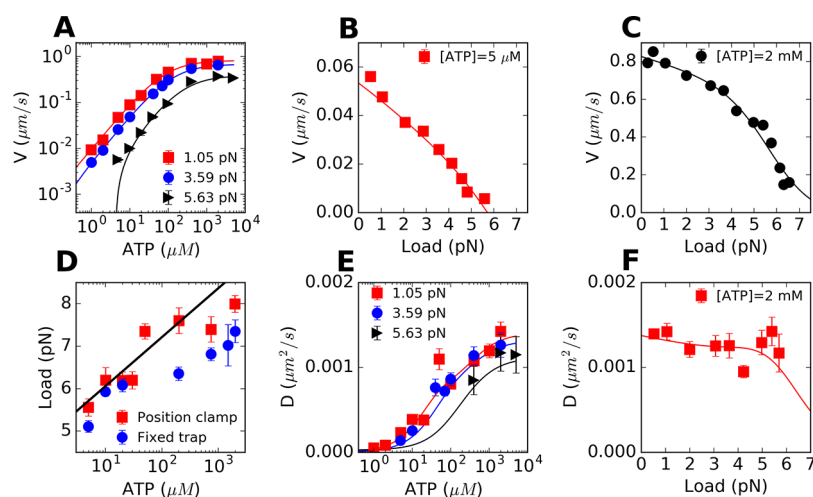


Figure 5. Analysis of experimental data, digitized from ref 33, using ($N = 4$)-state cyclic model. The solid lines are the fits to the data. (A) V vs $[ATP]$ at $f = 1.05$ pN (red square), 3.59 pN (blue circle), and 5.63 pN (black triangle). (B) V vs f at $[ATP] = 5 \mu\text{M}$. (C) V vs f at $[ATP] = 2 \text{ mM}$. (D) Stall force as a function of $[ATP]$, measured by “Position clamp” (red square) or “Fixed trap” (blue circle) methods. (E) D vs $[ATP]$ at $f = 1.05$ pN (red square), 3.59 pN (blue circle), and 5.63 pN (black triangle). D was estimated from $r = 2D/Vd_0$. (F) D vs f at $[ATP] = 2 \text{ mM}$.

philosophy underlying the analysis of mapping trajectories on the kinetic model, proposed here on kinesin-1 as well as others on F_1 -ATPase,^{29,46} is in essence similar to the one by the recent study which has quantified circulating flux on configurational phase space (or mode space) to diagnose broken DB and nonequilibrium dynamics at the mesoscopic scale.^{37,38} Lastly, our study confers quantitative insights into how much of the chemical free energy supplied to active systems (enzymes, molecular motors) is converted to mechanical movement in space and eventually dissipated into heat. Variations in the transport properties and heat dissipation among different molecular motors provides glimpses into their design principles,⁴⁷ which should also be highlighted against typical enzymes specialized for catalysis.

COMPUTATIONAL METHODS

Analysis of Kinesin-1 Data Using ($N = 4$)-State Kinetic Model. The data digitized from ref 33 were fitted to the ($N = 4$)-state model used by Fisher and Kolomeisky,²¹ but we kept the parameter w_4 independent of $[ATP]$. Initial values for the fit were chosen from eqs 14 and 15 in ref 21, except that we set $w_4 = 100 \text{ s}^{-1}$ as an initial value for the fit. The *curve_fit* from *scipy*⁴⁸ was used to globally fit the data in Figures 2A–C and 5A–F. θ_4^- is determined from the constraint $\sum_{n=1}^N (\theta_n^+ + \theta_n^-) = 1^{20}$ at every iteration step. The parameters determined from the fit shown in Figure 5 are provided in Table 2, and they are comparable to those in ref 21.

Table 2. Parameters Determined from the Fit Using ($N = 4$)-State Model^a

u_1^0	2.3	u_2	600	u_3	400	u_4	190
θ_1^+	0.00	θ_2^+	0.04	θ_3^+	0.01	θ_4^+	0.02
w_1	20	w_2	1.4	w_3	1.7	w_4	120
θ_1^-	0.14	θ_2^-	0.15	θ_3^-	0.5	θ_4^-	0.14

^aThe unit of $\{u_n\}$ and $\{w_n\}$ is s^{-1} except for u_1^0 ($[u_1^0] = \mu\text{M}^{-1} \text{ s}^{-1}$).

ASSOCIATED CONTENT

Supporting Information

The Supporting Information is available free of charge on the ACS Publications website at DOI: 10.1021/acs.jpclett.6b02657.

- (1) Derivation of the third-degree polynomial dependence of D on V ;
- (2) 1D hopping model with a finite processivity;
- (3) mapping the master equation for N -state kinetic model onto Langevin and Fokker–Plank equations;
- (4) nonequilibrium steady-state thermodynamics;
- (5) relationship between motor diffusivity and heat dissipation;
- (6) rate constants, enhancement of diffusion, and conversion efficiency determined from the ($N = 2$)-state kinetic model; Figures S1–S3 (PDF)

AUTHOR INFORMATION

Corresponding Author

*E-mail: hyeoncb@kias.re.kr.

ORCID

Changbong Hyeon: 0000-0002-4844-7237

Notes

The authors declare no competing financial interest.

ACKNOWLEDGMENTS

We thank Bae-Yeun Ha, Hyunggyu Park, Dave Thirumalai, and Anatoly Kolomeisky for helpful comments and illuminating discussions. We acknowledge the Center for Advanced Computation in KIAS for providing computing resources.

REFERENCES

- (1) Muddana, H. S.; Sengupta, S.; Mallouk, T. E.; Sen, A.; Butler, P. J. Substrate Catalysis Enhances Single-Enzyme Diffusion. *J. Am. Chem. Soc.* **2010**, *132*, 2110–2111.
- (2) Yu, H.; Jo, K.; Kounovsky, K. L.; de Pablo, J. J.; Schwartz, D. C. Molecular Propulsion: Chemical Sensing and Chemotaxis of DNA Driven by RNA Polymerase. *J. Am. Chem. Soc.* **2009**, *131*, 5722–5723.
- (3) Sengupta, S.; Dey, K. K.; Muddana, H. S.; Tabouillot, T.; Ibele, M. E.; Butler, P. J.; Sen, A. Enzyme molecules as nanomotors. *J. Am. Chem. Soc.* **2013**, *135*, 1406–1414.

- (4) Sengupta, S.; Spiering, M. M.; Dey, K. K.; Duan, W.; Patra, D.; Butler, P. J.; Astumian, R. D.; Benkovic, S. J.; Sen, A. DNA Polymerase as a Molecular Motor and Pump. *ACS Nano* **2014**, *8*, 2410–2418.
- (5) Riedel, C.; Gabizon, R.; Wilson, C. A. M.; Hamadani, K.; Tsekouras, K.; Marqusee, S.; Presse, S.; Bustamante, C. The heat released during catalytic turnover enhances the diffusion of an enzyme. *Nature* **2015**, *517*, 227–230.
- (6) Golestanian, R. Enhanced Diffusion of Enzymes that Catalyze Exothermic Reactions. *Phys. Rev. Lett.* **2015**, *115*, 108102.
- (7) Bai, X.; Wolynes, P. G. On the hydrodynamics of swimming enzymes. *J. Chem. Phys.* **2015**, *143*, 165101.
- (8) Tsekouras, K.; Ridel, C.; Gabizon, R.; Marqusee, S. P.; Bustamante, C. Comment on “Enhanced Diffusion of Enzymes that Catalyze Exothermic Reactions” by R. Golestanian. 2016, arXiv:1608.05433v1. <https://arxiv.org/abs/1608.05433>
- (9) Golestanian, R. Reply to Comment on “Enhanced diffusion of enzymes that catalyze exothermic reactions”. 2016, arXiv:1608.07469v1. <https://arxiv.org/abs/1608.07469>.
- (10) Visscher, K.; Schnitzer, M. J.; Block, S. M. Single kinesin molecules studied with a molecular force clamp. *Nature* **1999**, *400*, 184–187.
- (11) Nishiyama, M.; Muto, E.; Inoue, Y.; Yanagida, T.; Higuchi, H. Substeps within the 8-nm step of the ATPase cycle of single kinesin molecules. *Nat. Cell Biol.* **2001**, *3*, 425–428.
- (12) Yildiz, A.; Tomishige, M.; Vale, R. D.; Selvin, P. R. Kinesin Walks Hand-over-Hand. *Science* **2004**, *303*, 676–678.
- (13) Carter, N. J.; Cross, R. A. Mechanics of the kinesin step. *Nature* **2005**, *435*, 308–312.
- (14) Yildiz, A.; Tomishige, M.; Gennerich, A.; Vale, R. D. Intramolecular Strain Coordinates Kinesin Stepping Behavior along Microtubules. *Cell* **2008**, *134*, 1030–1041.
- (15) Dey, K. K.; Zhao, X.; Tansi, B. M.; Méndez-Ortiz, W. J.; Córdova-Figueroa, U. M.; Golestanian, R.; Sen, A. Micromotors Powered by Enzyme Catalysis. *Nano Lett.* **2015**, *15*, 8311–8315.
- (16) Hyeon, C.; Onuchic, J. N. Mechanical control of the directional stepping dynamics of the kinesin motor. *Proc. Natl. Acad. Sci. U. S. A.* **2007**, *104*, 17382–17387.
- (17) Zhang, Z.; Thirumalai, D. Dissecting the kinematics of the kinesin step. *Structure* **2012**, *20*, 628–640.
- (18) Schnitzer, M. J.; Block, S. M. Kinesin hydrolyses one ATP per 8-nm step. *Nature* **1997**, *388*, 386–390.
- (19) Derrida, B. Velocity and diffusion constant of a periodic one-dimensional hopping model. *J. Stat. Phys.* **1983**, *31*, 433–450.
- (20) Fisher, M. E.; Kolomeisky, A. B. The force exerted by a molecular motor. *Proc. Natl. Acad. Sci. U. S. A.* **1999**, *96*, 6597–6602.
- (21) Fisher, M. E.; Kolomeisky, A. B. Simple mechanochemistry describes the dynamics of kinesin molecules. *Proc. Natl. Acad. Sci. U. S. A.* **2001**, *98*, 7748–7753.
- (22) Oono, Y.; Paniconi, M. Steady state thermodynamics. *Prog. Theor. Phys. Suppl.* **1998**, *130*, 29–44.
- (23) Hatano, T.; Sasa, S. Steady-state thermodynamics of Langevin systems. *Phys. Rev. Lett.* **2001**, *86*, 3463–3466.
- (24) Hyeon, C.; Klumpp, S.; Onuchic, J. N. Kinesin’s backsteps under mechanical load. *Phys. Chem. Chem. Phys.* **2009**, *11*, 4899–4910.
- (25) Qian, H.; Beard, D. A. Thermodynamics of stoichiometric biochemical networks in living systems far from equilibrium. *Biophys. Chem.* **2005**, *114*, 213–220.
- (26) Qian, H. Phosphorylation Energy Hypothesis: Open Chemical Systems and Their Biological Functions. *Annu. Rev. Phys. Chem.* **2007**, *58*, 113–142.
- (27) Qian, H. A simple theory of motor protein kinetics and energetics. II. *Biophys. Chem.* **2000**, *83*, 35–43.
- (28) Qian, H. Motor protein with nonequilibrium potential: Its thermodynamics and efficiency. *Phys. Rev. E* **2004**, *69*, 012901.
- (29) Toyabe, S.; Okamoto, T.; Watanabe-Nakayama, T.; Taketani, H.; Kudo, S.; Muneyuki, E. Nonequilibrium Energetics of a Single F1-ATPase Molecule. *Phys. Rev. Lett.* **2010**, *104*, 198103.
- (30) Qian, M.; Zhang, X.; Wilson, R. J.; Feng, J. Efficiency of Brownian motors in terms of entropy production rate. *EPL (Europhysics Letters)* **2008**, *84*, 10014.
- (31) Hyeon, C.; Onuchic, J. N. A Structural Perspective on the Dynamics of Kinesin Motors. *Biophys. J.* **2011**, *101*, 2749–2759.
- (32) Klumpp, S.; Lipowsky, R. Active Diffusion of Motor Particles. *Phys. Rev. Lett.* **2005**, *95*, 268102.
- (33) Visscher, K.; Schnitzer, M. J.; Block, S. M. Single kinesin molecules studied with a molecular force clamp. *Nature* **1999**, *400*, 184–189.
- (34) Kalnin, J. R.; Berezhkovskii, A. M. Note: On the relation between Lifson-Jackson and Derrida formulas for effective diffusion coefficient. *J. Chem. Phys.* **2013**, *139*, 196101.
- (35) Liepelt, S.; Lipowsky, R. Kinesin’s network of chemomechanical motor cycles. *Phys. Rev. Lett.* **2007**, *98*, 258102.
- (36) Clancy, B.; Behnke-Parks, W.; Andreasson, J.; Rosenfeld, S.; Block, S. A universal pathway for kinesin stepping. *Nat. Struct. Mol. Biol.* **2011**, *18*, 1020–1027.
- (37) Battle, C.; Broedersz, C. P.; Fakhri, N.; Geyer, V. F.; Howard, J.; Schmidt, C. F.; MacKintosh, F. C. Broken detailed balance at mesoscopic scales in active biological systems. *Science* **2016**, *352*, 604–607.
- (38) Gladrow, J.; Fakhri, N.; MacKintosh, F. C.; Schmidt, C. F.; Broedersz, C. P. Broken Detailed Balance of Filament Dynamics in Active Networks. *Phys. Rev. Lett.* **2016**, *116*, 248301.
- (39) Tailleur, J.; Cates, M. E. Statistical Mechanics of Interacting Run-and-Tumble Bacteria. *Phys. Rev. Lett.* **2008**, *100*, 218103.
- (40) Liu, C.; Fu, X.; Liu, L.; Ren, X.; Chau, C. K.; Li, S.; Xiang, L.; Zeng, H.; Chen, G.; Tang, L. H.; et al. Sequential establishment of stripe patterns in an expanding cell population. *Science* **2011**, *334*, 238–241.
- (41) Condat, C. A.; Jäcke, J.; Menchón, S. A. Randomly curved runs interrupted by tumbling: A model for bacterial motion. *Phys. Rev. E* **2005**, *72*, 021909–7.
- (42) Lovely, P. S.; Dahlquist, F. Statistical measures of bacterial motility and chemotaxis. *J. Theor. Biol.* **1975**, *50*, 477–496.
- (43) Mizuno, D.; Tardin, C.; Schmidt, C.; MacKintosh, F. Nonequilibrium mechanics of active cytoskeletal networks. *Science* **2007**, *315*, 370–373.
- (44) Marchetti, M.; Joanny, J.; Ramaswamy, S.; Liverpool, T.; Prost, J.; Rao, M.; Simha, R. A. Hydrodynamics of soft active matter. *Rev. Mod. Phys.* **2013**, *85*, 1143.
- (45) Wu, M.; Roberts, J. W.; Kim, S.; Koch, D. L.; DeLisa, M. P. Collective Bacterial Dynamics Revealed Using a Three-Dimensional Population-Scale Defocused Particle Tracking Technique. *Appl. Environ. Microbiol.* **2006**, *72*, 4987–4994.
- (46) Shinagawa, R.; Sasaki, K. Enhanced Diffusion of Molecular Motors in the Presence of Adenosine Triphosphate and External Force. *J. Phys. Soc. Jpn.* **2016**, *85*, 064004–9.
- (47) Hinczewski, M.; Tehver, R.; Thirumalai, D. Design principles governing the motility of myosin V. *Proc. Natl. Acad. Sci. U. S. A.* **2013**, *110*, E4059–E4068.
- (48) Jones, E.; Oliphant, T.; Peterson, P. SciPy: Open source scientific tools for Python. <http://www.scipy.org/>, 2001–.